

Observed directional characteristics of the wind, wind stress, and surface waves on the open ocean

Karl F. Rieder and Jerome A. Smith

Scripps Institution of Oceanography, La Jolla, CA 92093-0213

Robert A. Weller

Woods Hole Oceanographic Institution, Woods Hole, MA 02543

Abstract. Sonic anemometer data were taken during the Surface Waves Processes Program (SWAPP) in March 1990 in the North Pacific. The measurements of wind stress vector span several strong wind events. Significant angles between the wind stress vector and the mean wind vector are seen. Simultaneous measurements of the directional wave field were made with a surface scanning Doppler sonar. The data suggest that the wind stress direction is influenced by the direction of the surface waves, especially for stronger winds. Overall, the stress vector lies between the mean wind and the mean wave directions. At the higher wind speeds (over 8.6 m/s), there is non-zero correlation between the variations in wave directions and stress directions as well. Finally, the stress and wave component directions have similar frequency dependence over the frequency band where wave energy is non-negligible, suggesting a dynamic link.

1. Introduction

The surface flux of momentum, or wind stress, influences all aspects of air-sea interactions. For example, it drives the growth of capillary and surface gravity waves, the development of the mixed layer, and even the large-scale circulation of the oceans. An improved understanding of the wind stress vector is of interest to meteorologists, oceanographers, and climatologists alike [Dobson and Toulany, 1991].

Wind stress is often estimated using a “bulk method,” in which the stress magnitude is assumed to be proportional to the square of the wind speed:

$$|\tau| = \rho C_d U^2, \quad (1)$$

where C_d is a drag coefficient. In practice, this drag coefficient is taken to depend on atmospheric stability and the height at which U is measured. The dependence on stability is usually cast in terms of a height dependent stability parameter, z/L , where L is the Monin-Obukov length [Monin and Obukov 1954, as cited in Businger *et al.* 1971]. Conceptually, L is a scale height for balancing buoyancy flux against wind stress. In practice, if the stress is to be estimated by the bulk method, so must the buoyancy flux. Corrections for different measurement heights are made assuming a logarithmic profile for the mean wind.

Dependence of the drag coefficient on wave state or surface roughness has also been considered [e.g., Hsu, 1974, Kitaigorodskii and Saslavsky, 1974, Donelan, 1982, Janssen, 1989]. In most analyses to date, the wind stress is still generally assumed to lie in the direction of the mean wind.

Given high-frequency three-dimensional wind components, a better estimate of the stress vector is given by

$$\rho^{-1} \tau = -\langle u'w' \rangle i - \langle v'w' \rangle j, \quad (2)$$

where u' , v' , and w' are the downwind, crosswind, and vertical fluctuating wind velocities respectively. Direct measurements of the wind stress vector are becoming increasingly common; however, the idea is fairly new, and a large portion of the historical data set is based on bulk formulae.

Somewhat unexpectedly, it has been found that the crosswind component $\langle v'w' \rangle$ can be non-zero, implying that the wind stress direction is different from that of the mean wind [Zemba and Friehe, 1987, Geernaert, 1988]. The angle between the stress and mean wind is given by

$$\theta = \tan^{-1}(\langle v'w' \rangle / \langle u'w' \rangle). \quad (3)$$

Zemba and Friehe (1987) observed large angles between the wind and stress, which they attributed in part to the existence of a coastal jet. Geernaert (1988) attributed 30% of the variance in this wind stress angle to the effect of the heat flux, for the data considered. He showed that the sign of the angle between the wind stress and the mean wind vectors varied with that of the stability parameter, z/L . The highest correlation with the wind stress angle (0.58) was with a “temperature flux” term, $U_{10}(T_0 - T_{10})$, where U_{10} is the wind speed at 10 m elevation, T_0 is the sea surface temperature, and T_{10} is the 10m air temperature. He suggested this is related to veering of the wind with height, and the redirection of the resulting bursts of momentum. Geernaert *et al.* [1993] also suggested that some of the remaining variance is due to the influence of the surface gravity wave field, finding that in general the wind stress lies between the mean wind direction and the direction of the long waves. While Geernaert was able to propose this hypothesis,

Copyright 1994 by the American Geophysical Union.

Paper number 94JC02215.
0148-0227/94JC-02215 \$05.00

his data set was limited and did not provide statistically significant results.

Here we consider further the influence of the surface wave directionality on wind stress direction with a larger data set and more extensive statistical analysis. Data were collected during the Surface Waves Processes Program (SWAPP), from February 24 through March 18 1990, on the research floating instrument platform, *FLIP*. During SWAPP, many instruments were deployed, including two 3-component sonic anemometers to measure the turbulent wind field, and a surface scanning Doppler sonar to measure surface wave directional spectra.

In section 2 the experimental program, data collection, and measurements are described. Data analysis is discussed in section 3. Results are presented in section 4. The effect of swell direction on the wind stress vector is studied, and the analysis is extended to comparisons on a frequency-by-frequency basis.

2. Experimental Program and Data Collection

The motivation for the SWAPP centers on understanding wave breaking and the interaction between surface waves and the upper ocean boundary layer. For SWAPP, the research platform *FLIP* was moored about 500 km west of Point Conception, at 35N 127W (Figure 1). Measurements of the surface gravity waves, mixed layer structure, and air-sea fluxes were made from *FLIP*, involving a variety of investigators [Weller *et al.*, 1991].

To measure the surface gravity waves, a specialized surface scanning Doppler sonar was deployed from the hull of *FLIP* (Figure 2; Pinkel and Smith 1987, Smith 1989). Four 195 kHz beams, each having 3 m resolution and reaching to 400 m range, were directed at 45° increments in azimuth. A “quick look analysis” [Sarpkaya, 1990] provides accurate directional wave spectra for wave periods between about 2 and 14 seconds. This method provides robust estimates from less than 15 minutes’ worth of data, and is most suitable for the present study.

Suitable measurements were made for estimating air-sea fluxes by both bulk and (for stress) direct methods. A vector-

averaging wind recorder (VAWR) was mounted atop *FLIP* (22 m above mean sea level) to measure mean wind velocities. Measurements of air temperature, relative humidity, and barometric pressure were also made. These data were averaged over 56.25-s intervals (1/64 hour), recorded, and used to make bulk estimates of the vertical flux of momentum and heat.

For direct measurement of the vertical flux of momentum, and to assist in estimates of heat and buoyancy fluxes, three-component sonic anemometers were deployed at the ends of both the port and aft booms, at 8 and 6 meters above mean sea level respectively. For example, an estimate of the stability parameter using $\langle T'w' \rangle$ from a sonic anemometer is given by Large and Pond (1981). Measurements of U , V , and W components of wind, and of sound speed (temperature), were taken ten times per second.

For this study, we use data from the sonic anemometer and accompanying instrumentation on the aft boom. This site was chosen since it was out of the lee of *FLIP* during the ten days examined here. The estimates of wind stress, velocity, and atmospheric stability all refer to a 6 meter elevation above the mean ocean surface.

3. Data Analysis

The sonic anemometer data were averaged to 2 Hz sample rate to reduce data size. Stress estimates were made every 30 minutes. To verify that the frequencies important to the stress estimate are included, we examined the integral of the $u'w'$ co-spectra (Figure 3) using data from a few representative segments. Most of the contribution is from frequencies between .01 and 1 (periods of 100 and 1 s respectively). The error incurred by reducing the data to 2 Hz is about 1% or less. Conversely, 30 minute averaging times provide more than 15 degrees of freedom at the lowest contributing frequencies.

A series of selection criteria was applied to the data. First, conditions during which wind speeds were less than 3 m/s are not considered. Second, to ensure reliable estimates of the angle between the mean wind and wind stress directions, estimates of the downwind stresses are required to be different from zero with a statistical confidence of 99%. Third, sheltering by *FLIP*'s structure was considered. Paulson *et al.* [1972] found a maximum error of about 5% in wind speed for anemometers mounted approximately 15 m from the hull of *FLIP*. However, stress measurements need to be analyzed further, and a criterion for selecting acceptable wind directions is needed. For all data satisfying the first two criteria, measured angles between the wind and stress directions are plotted in Figure 4 against the angle between the wind direction and the aft boom of *FLIP* (0° on the horizontal axis corresponds to the boom pointing directly upwind; -90° represents winds perpendicular to the aft boom). When the sonic anemometer is partially sheltered by *FLIP*, large angles between the wind and stress directions are seen, particularly during low wind speed conditions (circles). These angles are so large as to be unphysical, with nearly opposing wind and stress directions. Therefore, for low wind speeds, only conditions with wind directions less than 70° off the boom were accepted. For higher winds, the criterion was relaxed to include conditions with relative directions less than 100°.

Finally, effects produced by the motion of *FLIP* and *FLIP*'s boom were analyzed and found to be insignificant. Tilts and velocities at the sites of the anemometers were estimated using a *FLIP* motion model, together with accelerometer, fluxgate,

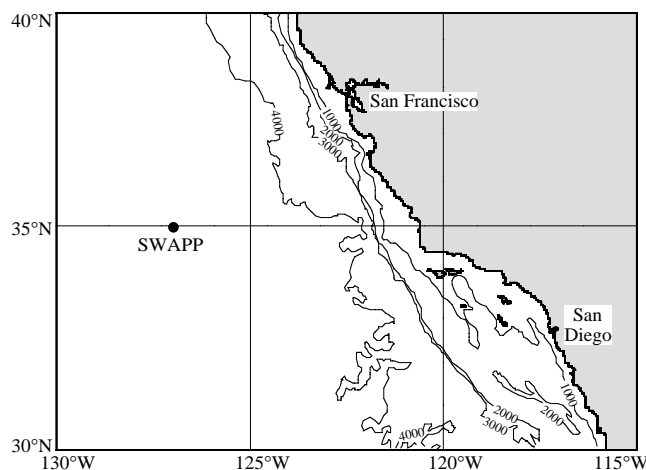


Figure 1. Location of the Surface Waves and Processes Program (SWAPP). The research platform *FLIP* was moored approximately 500 km west of Point Conception at 35N, 127W. Contours in meters.

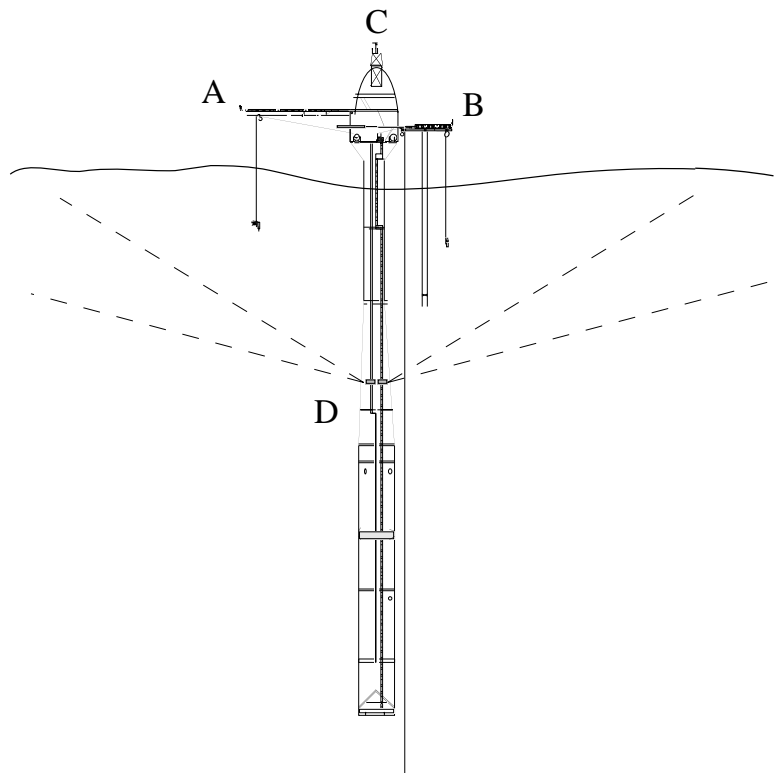


Figure 2. Schematic view of R/P *FLIP* during SWAPP experiment. Instruments deployed included: (A and B) high frequency sonic anemometers; (C) vector-averaging wind recorder (VAWR) and (D) surface scanning Doppler sonars.

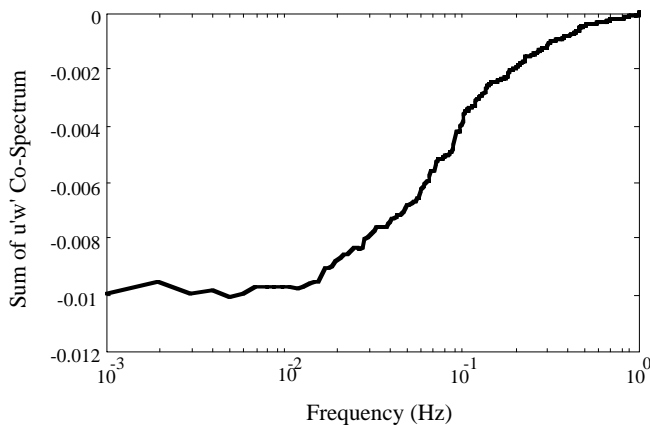


Figure 3. The cumulative sum of $u'w'$ co-spectra from high to low frequencies, from a typical sonic anemometer data run. Virtually all energy is contained between frequencies of 0.01 and 1 (periods of 100 and 1 s, respectively).

and gyroscope (heading) measurements. It was found that the induced wind stress is typically two to three orders of magnitude smaller than the stress estimates from the sonic anemometer data.

Figure 5 shows wind speed, downwind and crosswind stresses, wind and wave directions, and *FLIP*'s heading for the portion of the observation period used in this study. Three significant wind maxima occurred during this period. In the

first event, the wind picked up quickly from calm conditions (including little swell), and veered only slightly in direction over the course of 30 hours. The second and third events were accompanied by varying sea conditions, with swell present at varying angles from the wind direction.

4. Results

One current hypothesis is that the surface gravity wave spectrum influences the direction of the mean stress vector by creating an anisotropic roughness field at the surface. This effect has been attributed to the redistribution of energy and slope density of the short waves, which are theorized to be the significant supporters of momentum flux from the atmosphere to the ocean [Byrne, 1982, Geernaert *et al.*, 1986]. The long waves strain the short ones, turning them (and hence the wind stress) toward the direction of the long waves or swell [Geernaert, *et al.*, 1993]. Here, we shall also consider hypotheses that this influence varies with wind speed (overall surface roughness has been theorized to increase with wind speed [Charnock, 1955]), and that the influence can be seen in a detailed examination by frequency.

4.1 Stress Direction versus Swell Direction

Figure 6 shows a plot of angles between the stress and wind directions (or “stress angles”) versus angles between swell and wind directions (or “swell angles”). All directions are calculated using the oceanographic convention (toward). Data are plotted only for neutral stability ($-0.1 < z/L < 0.1$, $z=6$ m),

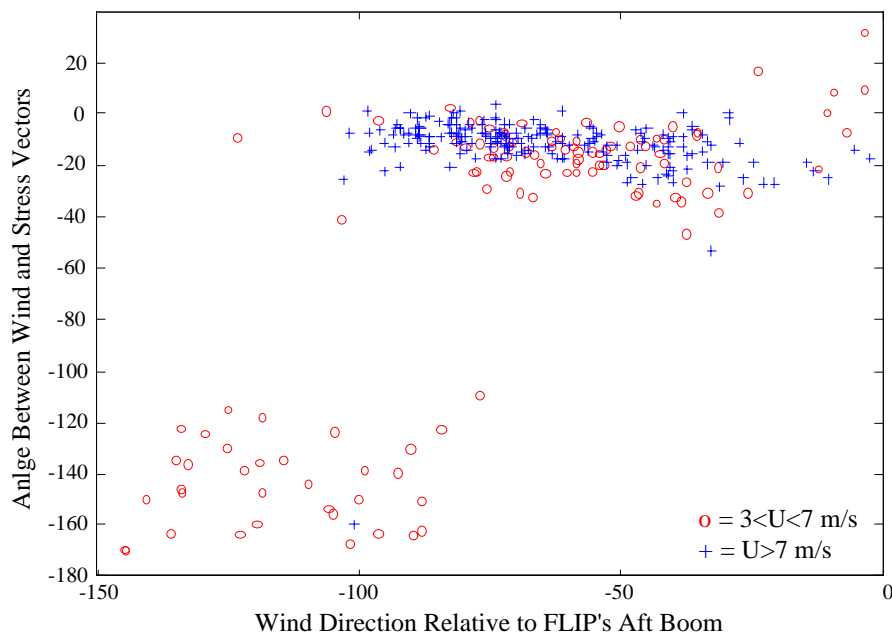


Figure 4. The angle between mean wind direction and the wind stress direction versus the wind direction relative to the aft boom of *FLIP* (0° means the aft boom points upwind). For cases in which the sonic anemometer is at least partially in the lee of the *FLIP* superstructure (particularly for low wind speeds), large (unphysical) absolute values of the angle between the mean wind and stress directions are seen.

to reduce the buoyancy flux effect described by Geernaert (1988). The data are further divided into high wind speed and low wind speed regimes, using the median observed wind speed of 8.6 m/s (yielding 58 samples in each regime). The data were already selected for winds above 3 m/s, and only one case lies below 5.8 m/s, so the low wind interval is roughly 6 to 8.6 m/s. The high wind interval is roughly 8.6 to 12 m/s (all at 6 m elevation). If the stress vector has a linear bias toward the swell direction, the overall trend would be from lower left to the upper right, through the origin. The centroid of the low wind data points is consistent with this, but there is no significant trend in the variations about the centroid. The high wind data support this in both mean and trend: for the high wind cases, the variations in stress angle about the mean is correlated with the corresponding variations in swell angle. The correlation squared is $C^2=0.21$, which is well above the 95% significance level of 0.05 (from 58 samples). In contrast, the low wind data yields a correlation squared of only $C^2=0.01$, which is not significantly different from zero. To illustrate this correlation, a line is drawn through the centroid of the high wind cases along the major axis of the joint variations. Error bars are provided by drawing dashed lines parallel to the major axis but displaced up and down by the RMS distance of the data from this line.

Caution should be exercised in deriving meaning from overall mean values, since these may be determined by effects such as the large scale structure of the wind field. However, the relatively good correlation between stress and swell angles for the high wind cases lends support to the hypothesis that the swell direction influences the stress.

4.2. Wind Speed Dependence

There is a slight suggestion in Figure 6 that the low wind speed cases (crosses) lie lower in the plot than the high wind

speed cases, on the average. To investigate this further, we divide the data into three bands of swell angles: -45° to -35° , -35° to -25° , and -25° to -15° . This should reduce the effect of varying swell directions on the direction of the stress, and so bring to light any modulation of this influence by the strength of the wind. Figure 7 shows the stress angle versus wind speed for these fixed bands of swell angles. The data suggest a dependence on wind speed for the middle band of angles, -35° to -25° . The correlation squared is 0.455, which is well above the 95% confidence level of 0.092 for an estimate based on 31 points. However, no significant correlation is seen in either the -45° to -35° band or the -25° to -15° band: the measured correlations squared are 0.072 (from 29 samples) in the high swell angle band, and 0.069 (from 23 samples) in the lowest swell angle band.

4.3. Frequency Analysis

In the above, the turning of the stress vector from the wind direction was compared with a “peak wave” or “swell” direction. Here, we pursue spectral descriptions of the stress and waves, hoping to shed light on further interdependencies. The direction of the stress as a function of frequency is estimated as

$$\theta(f) = \tan^{-1}(C_{v'w'}/C_{u'w'}), \quad (4)$$

where $C_{v'w'}$ and $C_{u'w'}$ are the co-spectra (the real parts of the cross-spectra) between the crosswind and vertical fluctuating velocities and the downwind and vertical fluctuating velocities, respectively. The wave directions are from the “quick analysis” of Doppler sonar data [Smith and Bullard, 1995]. Figures 8 and 9 show the directions and magnitudes of the stress and surface waves versus frequency. The two time periods (1000-1600 UTC March 8, and 0800-1400 March

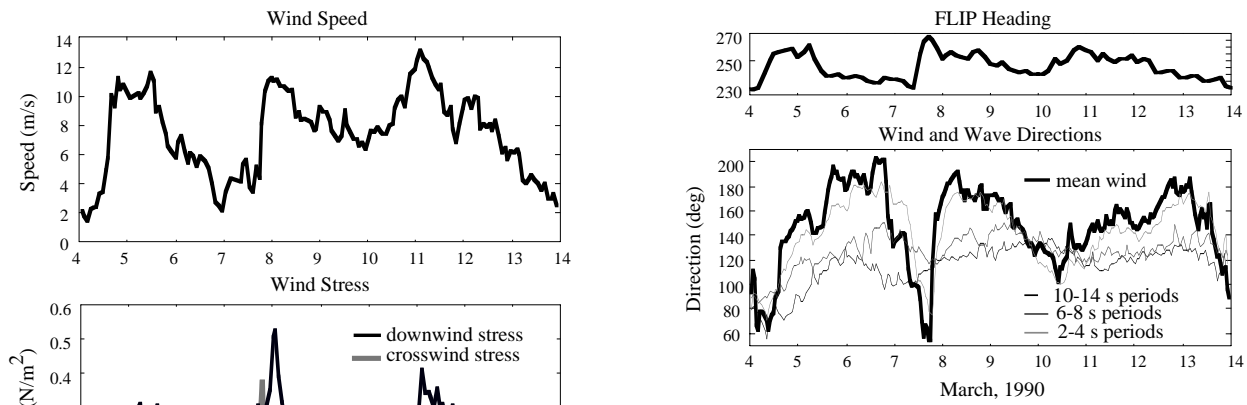


Figure 5. Wind speed, downwind and crosswind stress, and mean wind and wave directions along with *FLIP* heading, during the ten day period of the SWAPP cruise used in this study. All wind measurements were made at 6 meter elevation. Three significant wind events can be seen starting on March 4, 7, and 10.

11, 1990) were chosen because each has a nearly constant angle between the swell and wind directions, and each occurred during periods of near neutral stability. The March 8 period had nearly constant swell and wind directions over the course of 6 hours, while the March 11 period had slow turning of both the wind and swell directions. Both periods comprise several hours, lending statistical confidence to the results. Horizontal to vertical velocity co-spectra were calculated using 52 minute

segments, which were then averaged together to form estimates of the stress angle versus frequency for each of the two periods. Wave directional spectra were formed from 12–min segments and averaged over the same time periods to obtain wave directions. For display, a least-squares-fit fifth-order polynomial is drawn through the data, regressed against the logarithm of frequency. This effectively averages the data over logarithmically increasing intervals as the frequency

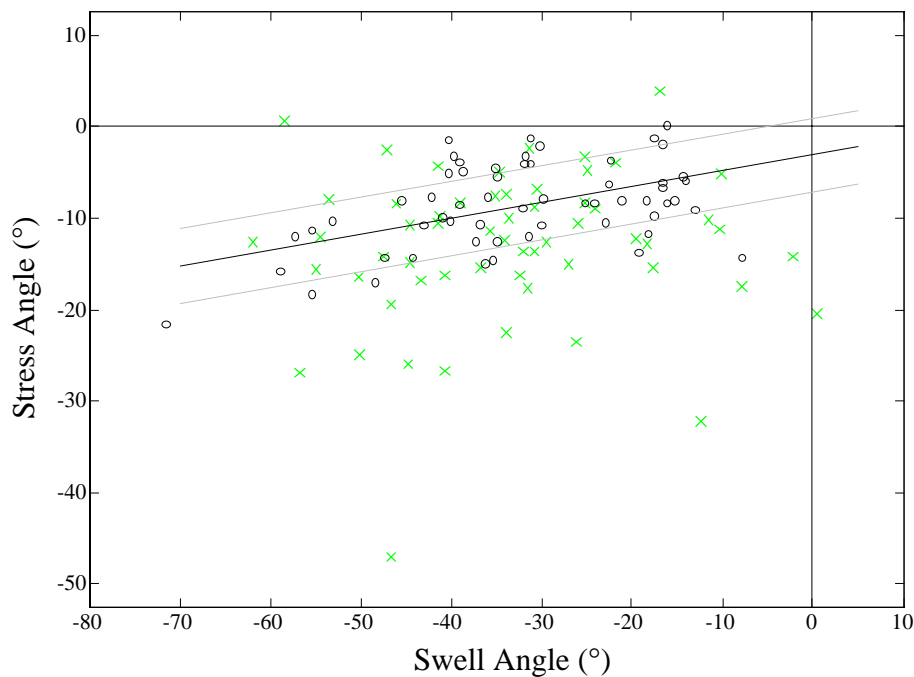


Figure 6. Angles between the stress and wind directions versus angles between swell and wind directions. Almost all points are in the third quadrant, indicating a tendency for the stress vector to align toward the swell direction from the wind direction. The data are divided into high wind (circles) and low wind (crosses) regimes. The major axis of the joint variations for the high wind cases only is illustrated by the straight line; the corresponding correlation squared is 0.21 (for the variations about the mean values). Error bounds (rms distance from the line) are indicated by dashed lines.

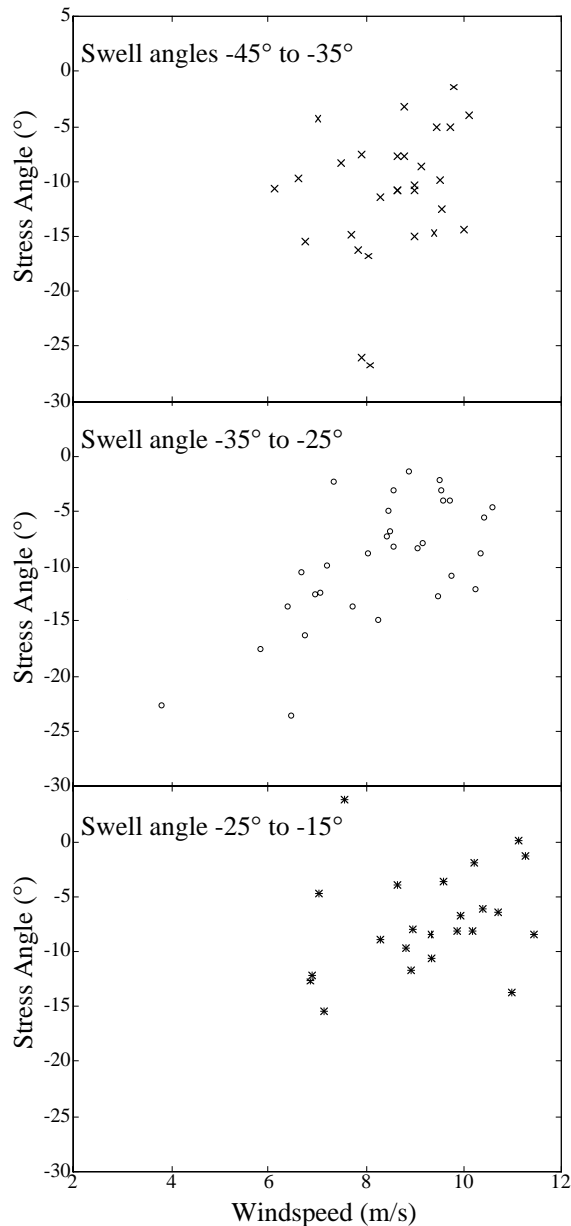


Figure 7. Stress angle versus wind speed (measured at 6 m height) for cases in which the swell angles are between -45° and -35° (top), between -35° and -25° (middle), or between -25° and -15° (bottom). A statistically significant trend with wind speed is seen in the middle plot.

increases. Only the data within the frequency band containing significant wave energy are included in the fits (0.05 to 0.5 Hz).

For the March 8 case, the wind is directed toward 193° , the net stress direction is toward 182° , and the swell direction is toward 140° . Thus, the stress direction lies between the swell and wind directions, as expected. Note that the higher frequency waves are more closely aligned with the mean wind direction. This is also as expected, since the higher frequency waves have a quicker response time to turning winds [Masson, 1990], and are locally generated. Somewhat unexpectedly, the variation with frequency of the stress direction mimics that of the surface gravity waves: the direction of the stress in the low-

frequency “swell regime” is aligned more closely with the direction of the waves at that frequency, and the direction of the wind stress at the high frequency “sea regime” is more closely aligned with the waves at those frequencies. (The scatter of points about the 5th order fit lines is a reasonable indicator of the statistical variability of the directional estimates.) This suggests that the fluctuations in the wind field at each frequency may be coupled to the fluctuations in the sea surface at the same frequencies.

The March 11 case exhibits similar results (Figure 9). Again, the stress direction lies between the wind and swell directions (132° versus 163° and 132° , respectively). However, in this case the stress is aligned more closely with the swell. Examining the directions versus frequency, a closer alignment of the wave and stress directions is seen. Surprisingly, the directions of the stresses lie even farther from the wind than the wave directions, over the whole “wave band” of frequencies. Again, the scatter of points about the polynomial fit is a good indicator of the statistical variability. As indicated in the lower portion of the Figures 8 and 9, most of the energy in the wind stress is contained in frequencies lower than those of the waves; however, there is strong evidence of

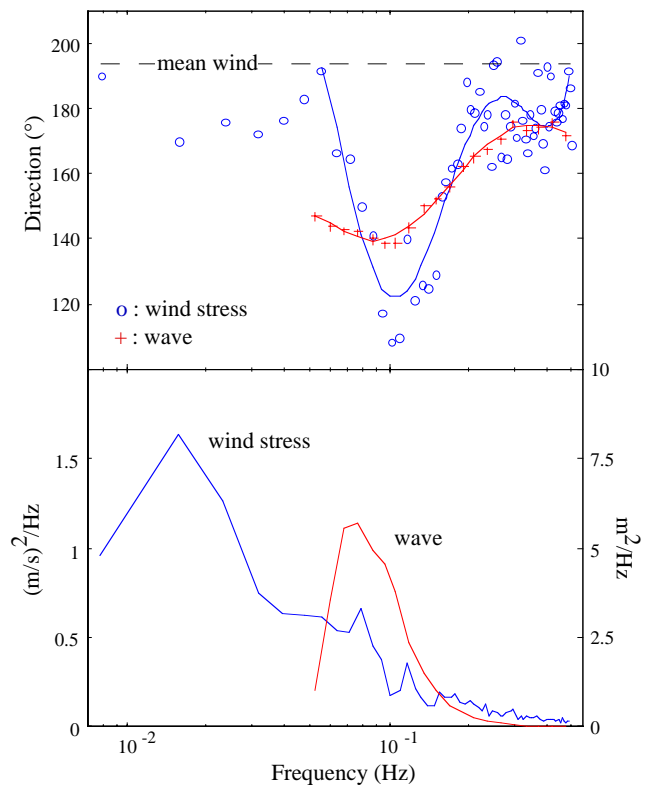


Figure 8. Direction (top) and magnitude (bottom) of stress and waves versus frequency for March 8, 1000–1600. Over a band of frequencies containing the waves (0.05 to 0.5 Hz), a 5th order polynomial was fit to the directions against the log of the frequency (solid line). This line effectively averages the data over logarithmically spaced intervals. The directional variations of stress and waves versus frequency are similar. Note that the low frequency stresses also lie between the wind direction (193°) and the direction of the long waves (140°). Waves with frequencies greater than .24 Hz have component wave ages less than 1.

an additive stress at the peak of the wave spectrum. Direct correlations between wind and wave components have been shown previously (e.g. Dobson, 1971; Elliott, 1972). Here, we are not showing direct correlations, but just a similarity in their directionality and spectral shapes.

5. Summary

Wind and wave data from SWAPP are used to explore relationships between the directions of the wind stress, mean wind, and wave field. These comparisons suggest that the direction of the wind stress vector is influenced by the direction of the surface gravity waves. The wind stress vector generally lies between the wind direction and the direction of the long waves, as found also by Geernaert (1993). For winds over 8.6 m/s, there is a significant trend in the observed stress angles versus swell angles, in a sense consistent with such an influence. Finally, the influence of the waves on the wind stress direction can be seen as a function frequency: the stress component directions as a function of frequency mimic the wave component directions, with both deviating from the mean wind.

The tracking in frequency of the wave and stress directions, in particular, suggests a dynamic link between the waves and

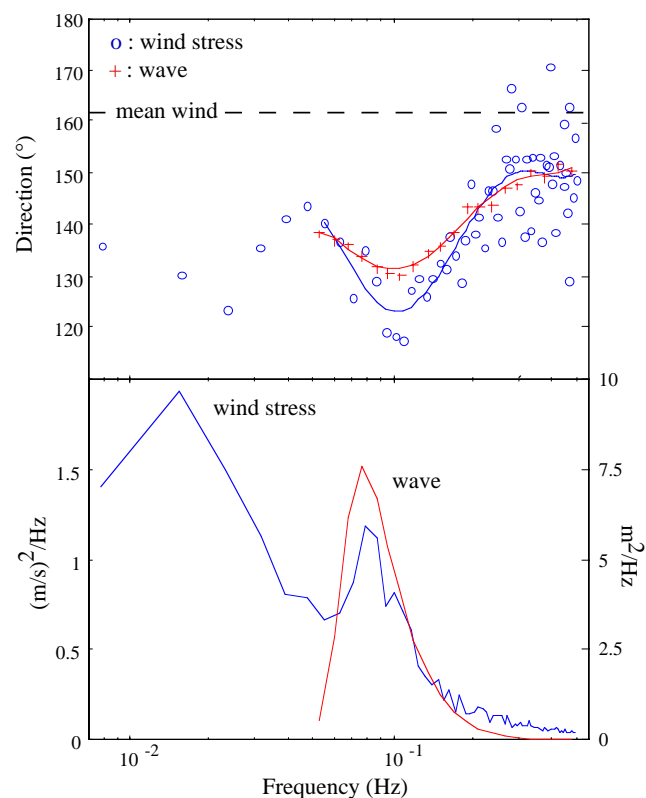


Figure 9. Direction (top) and magnitude (bottom) of wind stress and waves versus frequency for March 11, 0800–1400. The curve and averaging are as for figure 8. The variations with frequency of the wind stress and wave directions are again similar. In this case, the low frequency stresses are closely aligned with the long waves (near 132°). Waves with frequencies greater than .19 Hz have component wave ages less than 1.

stress. We hope to explore this further in future work, including data from different wind and wave conditions.

Acknowledgments. We thank Dr. Al Plueddemann of WHOI for his assistance in making the measurements on *FLIP* and Dr. Bruce Baker, NOAA, who loaned us one of the two sonic anemometers and checked the performance of both in a wind tunnel. Dr. Richard J. Seymour of SIO is also thanked for his advice, encouragement, and support. This work was supported by the PO division of the Office of Naval Research, under contracts N00014-90-J-1285 and N00014-93-1-0359. Additionally, this work is a result of research sponsored in part by NOAA, National Sea Grant College Program, Department of Commerce, under grant number NA89AA-D-SG138, project number R/OE-14, through the California Sea Grant College, and in part by the California Resources Agency. The U.S. Government is authorized to reproduce and distribute for governmental purposes.

References

- Businger, J. A., J. C. Wyngaard, Y. Izumi, and E. F. Bradley, Flux-Profile Relationships in the Atmospheric Boundary Layer, *Journal of the Atmospheric Sciences*, 28, 181-189, 1971.
- Byrne, H. M., The Variation of the Drag Coefficient in the Marine Surface Layer Due to Temporal and Spatial Variations of the Wind and Sea State, Ph.D. dissertation, University of Washington, Seattle, 1982.
- Charnock, H., Wind Stress on a Water Surface, *Quart. J. Roy. Meteor. Soc.*, 81, 639-640, 1955.
- Dobson, F., and B. Toulany, On the Wind-Wave Coupling Problem, in *Directional Ocean Wave Spectra*, Edited by Robert C. Beal, pp. 22-29, The John Hopkins University Press, Baltimore, 1991.
- Donelan, M. A., The Dependence of the Aerodynamic Drag Coefficient on Wave Parameters, paper presented at First International Conference on Meteorology and Air/Sea Interaction of the Coastal Zone, American Meteorological Society, The Hague, Netherlands, 1982.
- Geernaert, G. L., Measurements of the Angle Between the Wind Vector and Wind Stress Vector in the Surface Layer Over the North Sea, *Journal of Geophysical Research*, 93, 8215-8220, 1988.
- Geernaert, G. L., F. Hansen, M. Courtney, and T. Herbers, Directional Attributes of the Ocean Surface Wind Stress Vector, *Journal of Geophysical Research*, 98, 16571-16582, 1993.
- Geernaert, G. L., K. B. Katsaros, and K. Richter, Variation of the Drag Coefficient and Its Dependence on Sea State, *Journal of Geophysical Research*, 91, 7667-7679, 1986.
- Hsu, S. A., A Dynamic Roughness Equation and Its Application to Wind Stress Determination at the Air-Sea Interface, *Journal of Physical Oceanography*, 4, 116-120, 1974.
- Janssen, P. A. E. M., Wave-Induced Stress and the Drag of Air Flow over Sea Wave, *J. Phys. Oceanogr.*, 19, 745-754, 1989.
- Kitaigorodskii, S. A., and M. M. Saslavsky, A Dynamical Analysis of the Drag Conditions at the Sea Surface, *Boundary-Layer Meteorology*, 6, 53-61, 1974.
- Large, W. G., and S. Pond, Open Ocean Momentum Flux Measurement in Moderate to Strong Winds, *Journal of Physical Oceanography*, 11, 324-336, 1981.
- Masson, D., Observations of the Response of Sea Waves to Veering Winds, *J. Phys. Oceanogr.*, 20, 1876-1885, 1990.
- Paulson, C. A., E. Leavitt, and R. G. Fleagle, Air-Sea Transfer of Momentum, Heat, and Water Determined from Profile Measurements During BOMEX, *Journal of Physical Oceanography*, 2, 487-497, 1972.
- Pinkel, R., and J. A. Smith, Open Ocean Surface Wave Measurement Using Doppler Sonar, *Journal of Geophysical Research*, 92, 12967-12973, 1987.
- Sarpkaya, T., Wave Forces on Cylindrical Piles, in *Ocean Engineering Science*, Edited by Bernard Le Mehaute, and Daniel M. Hanes, pp. 169-194, John Wiley and Sons, Inc., New York, 1990.
- Smith, J. A., Doppler Sonar and Surface Waves: Range and Resolution, *J. Atm. and Ocean. Tech.*, 6, 680-696, 1989.

- Smith, J. A., and G. T. Bullard, Directional Surface Wave Estimates from Doppler Sonar Data, *Journal of Atmospheric and Oceanic Technology*, 12, 617-632, 1995.
- Weller, R. A., M. A. Donelan, M. G. Briscoe, and N. E. Huang, Riding the Crest: A Tale of Two Wave Experiments, *Bull. Amer. Meteor. Soc.*, 72, 163-183, 1991.
- Zemba, J., and C. A. Friehe, The Marine Atmospheric Boundary Layer Jet in the Coastal Ocean Dynamics Experiment, *Journal of Geophysical Research*, 92, 1489-1496, 1987.
-
- K. F. Rieder and J. A. Smith, Scripps Institution of Oceanography, La Jolla, CA 92093-0213. (e-mail: jasmith@ucsd.edu)
- R. A. Weller, Woods Hole Oceanographic Institution, Woods Hole, MA 02543. (e-mail: rweller@whoi.edu)
- (Received June 2, 1994; revised August 25, 1994; accepted August 25, 1994.)